

Impact of single pMOSFET dielectric degradation on NAND circuit performance

D. Estrada^a, M.L. Ogas^a, R.G. Southwick III^a, P.M. Price^b,
R.J. Baker^a, W.B. Knowlton^{a,b,*}

^a *Electrical and Computer Engineering Department, Boise State University, 1910 University Dr., Boise, ID 83725, USA*

^b *Materials Science and Engineering Department, Boise State University, 1910 University Dr., Boise, ID 83725, USA*

Received 17 July 2007; received in revised form 20 September 2007

Abstract

Degradation of CMOS NAND logic circuits resulting from dielectric degradation of a single pMOSFET using constant voltage stress has been examined by means of a switch matrix technique. As a result, the NAND gate rise time increases by greater than 65%, which may lead to timing errors in high frequency digital circuits. In addition, the NAND gate DC switching point voltage shifts by nearly 11% which may be of consequence for analog or mixed signal applications. Experimental results for the degraded pMOSFET reveal a decrease in drive current by approximately 43%. There is also an increase in threshold voltage by 23%, a decrease in source-to-drain conductance of 30%, and an increase in channel resistance of about 44%. A linear relationship between the degradation of the pMOSFET channel resistance and the increase in NAND gate rise time is demonstrated, thereby providing experimental evidence of the impact of a single degraded pMOSFET on NAND circuit performance.

© 2007 Elsevier Ltd. All rights reserved.

1. Introduction

The effects of dielectric breakdown mechanisms on inverter circuit performance have received recent attention [1–8], yet experimental results (i.e., not simulated) on these effects on other logic gates, such as the NAND gate, are negligible. Furthermore, the focus of reliability studies on the inverter logic circuit has involved the detrimental aspects of a circuit level stress on the DC voltage transfer characteristics (VTC) exclusive of circuit response in the time-domain [1,2,7,8]. In these studies, the type of degradation induced in one or both of the MOSFETs can only be inferred as electrical access to each individual MOSFET was not possible. However, it has been shown that directly characterizing each individual MOSFET before and after stress is possible by employing a switch matrix technique when configuring simple integrated circuit building blocks (SICBBs) [3,6]. This method

has been used to investigate inverter logic circuit performance following degradation of a single MOSFET (or both MOSFETs) [4] in which degradation of MOSFET parameters was examined and directly correlated to inverter degradation in the voltage–time-domain ($V-t$). The switch matrix technique has also been employed in a preliminary investigation on the degradation of rise time (t_r) in the NAND gate [9]. This study expands the preliminary investigation of NAND gate performance following pMOSFET degradation by comparing NAND circuit degradation in the DC and $V-t$ domains. Additionally, the correlation between pMOSFET degradation and NAND circuit reliability is experimentally and mathematically investigated. Moreover, the capacitive load associated with the switch matrix technique is addressed using experimental, mathematical, and simulation approaches.

Ogas et al. have proposed circuit performance can deteriorate before traditional gate oxide breakdown (GOB) events occur such as soft breakdown (SBD) or hard breakdown (HBD) [4]. Similarly, NAND gate and full adder

* Corresponding author. Tel.: +1 208 426 5705.

E-mail address: knowlton@boisestate.edu (W.B. Knowlton).

circuit simulations performed by Carter et al. suggest that logic circuits are affected dynamically by gate oxide degradation [10]. Their analyses present data that result in timing delays of NAND circuits and propagation of these timing delays through the logic path of a full adder circuit following a progressive GOB [10]. In addition, Hawkins et al. suggest IC parameter variance becomes a greater concern for the timing of logic circuits with the scaling of technology nodes through their simulations of NAND logic circuits [11]. However, to the authors' knowledge, experimental studies to support these simulations have yet to be performed on devices with ultra-thin oxides.

It is well known that device speed increases as MOSFET gate dielectric thickness (t_{OX}) is scaled down. However, with scaling, detrimental effects resulting in earlier dielectric breakdown, such as increased gate leakage current and increased defect generation become a greater concern. Consequently, it has become increasingly important to identify which components are most susceptible to dielectric degradation as circuit engineers continue to design with devices utilizing thinner gate oxides. Our study investigates the NAND logic circuit performance following degradation of devices with t_{OX} of 2.0 nm. Of particular interest is the reliability assessment of low-level oxide degradation (e.g., negative bias temperature instability [12,13], time dependent dielectric breakdown [14], stress induced leakage current [15], progressive breakdown [16,17], etc.), termed wear out in this paper [18], which may provide insight as to the critical degradation limit for digital circuit failure. This paper examines the effect of wear out in one pMOSFET on NAND gate performance. The focus of this study is not on the identity of the specific physical degradation mechanism (e.g., NBTI [12,13], TDDB [14], SILC [15] or progressive breakdown [16,17], etc.), which is left to the discretion of the reader, but on the impact of the induced device degradation on the NAND circuit response. To this end, a possible connection between MOSFET degradation and circuit performance may be established through the widely used relationship between circuit t_r and MOSFET channel resistance, R_{ch} , in the design of logic circuits, given by:

$$t_r \propto R_{ch} C_L \quad (1)$$

where C_L is the load capacitance on the logic circuit [19,20]. Based on our investigation of Eq. (1), we provide experimental evidence that directly correlates gate oxide wear out effects on the channel resistance of one pMOSFET to the NAND logic circuit rise time.

2. Experimental

2.1. Devices and measurements

The metal oxide semiconductor (MOS) devices used in this study are fabricated using 0.1 μm CMOS technology with a t_{OX} of 2.0 nm. The pMOSFET and nMOSFET devices configured in the NAND circuit have an oxide area

(A_{OX}) of $1 \times 10^{-8} \text{ cm}^2$ with a width and length of 10 μm and 0.1 μm , respectively. The dielectric type is SiO_2 . Measurements are obtained using a semiconductor characterization system described in previous studies [6]. Dielectric degradation is induced in a single pMOSFET by applying a constant voltage stress (CVS) of -4 V to the gate of the device (Fig. 1) [21]. Further description of the measurement and choice of applied voltage is reported in previous work [4]. CVS occurs in cycles of 600 s for five consecutive cycles, with interruptions for device and circuit characterization. The remaining three MOSFETs are not stressed. All measurements are conducted at 298 K.

Data have been collected and analyzed for 6 NAND gates with a single degraded pMOSFET configured in 1 of 2 positions through the switch matrix technique, as illustrated in Fig. 2. Table 1 summarizes all four NAND logic configurations, which are labeled with the pMOSFET position followed by the I/O state. Configurations 1–3 and 2–1, shaded in Table 1, correspond to transitions in the NAND logic. The results are presented for these two configurations in which device degradation affects the circuit performance in the voltage–time-domain ($V-t$). Specific to the NAND circuit, $V-t$ data and voltage transfer characteristics (VTCs) are measured following each stress cycle. The $V-t$ results allow for the evaluation of rise time (t_r) by taking the difference in time from 90% to 10% of the output voltage [20].

Data collected for the degraded pMOSFET includes maximum drain current ($I_{D,max}$), threshold voltage (V_{TH}), maximum transconductance ($G_{M,max}$), off-current (I_{off}), and small-signal source-to-drain conductance (g_{sdm}). The

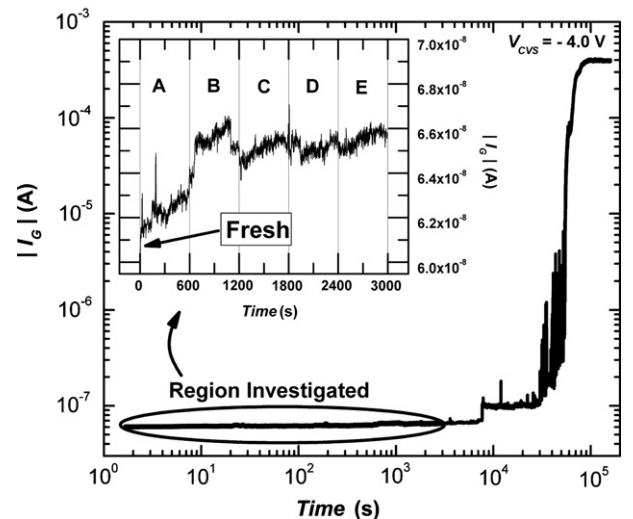


Fig. 1. CVS results showing gate current versus time of a pMOSFET with stress voltage, $V_G = -4.0 \text{ V}$. Wear out is in the low-leakage regime indicated by the Region Investigated, prior to the later breakdown events. The pMOSFETs used in this study were not stressed beyond the Region Investigated (i.e., 3000 s). An expanded view of the Region Investigated is shown in the inset and illustrates the five 600s stress cycles, A–E. The CVS measurement was interrupted following each stress cycle and circuit and device characteristics were obtained.

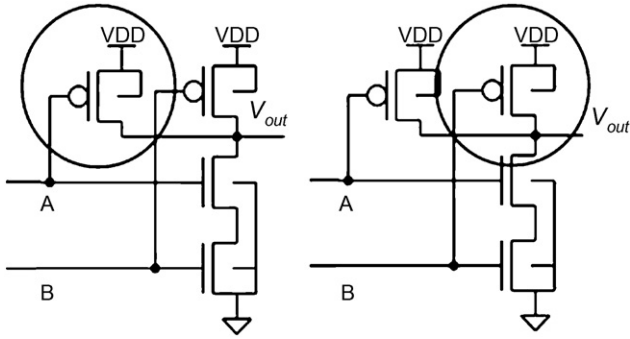


Fig. 2. NAND logic circuits illustrating positions 1 and 2 of the degraded pMOSFET. Following each stress cycle circuit characteristics were collected with the degraded pMOSFET in position 1 followed by collection of circuit characteristics with the degraded pMOSFET in position 2.

Table 1
NAND logic configurations^a indicating position and I/O state

pMOSFET position	Input/output state				
		1	2	3	4
1	Input A	VDD	GND	Pulsed	Pulsed
	Input B	Pulsed	Pulsed	VDD	GND
	Output	Pulsed	1	Pulsed	1
2	Input A	VDD	GND	Pulsed	Pulsed
	Input B	Pulsed	Pulsed	VDD	GND
	Output	Pulsed	1	Pulsed	1

^a NAND logic configurations are labeled with the pMOSFET position followed by the I/O state. Circuit configurations highlighted in bold indicate where single pMOSFET degradation affects the circuit response.

pMOSFET V_{TH} is determined using the linear extrapolation technique [22]. In addition, gate leakage current (I_{G-V_G}) is measured following each stress cycle. The g_{sdm} data are collected using a small-signal conductance measurement similar to that described by Kong et al. [23]. The small-signal conductance measurement used in this study differs from the method of Kong et al. in that a 14 mV RMS test signal at 1 MHz is applied to the drain of the device under test, while the voltage sources of the Agilent 4156C parameter analyzer provide the gate and substrate biases through connections configured using the Agilent E5250A switch matrix.

2.2. Switch matrix technique

The combination of equipment used for the switch matrix technique creates a significant capacitive load, which is typically a concern when dealing with small scale devices. The speed of small scale devices is critical to achieve high circuit performance and can easily be inhibited by the capacitive load due to charging effects. In a typical IC, several types of digital or mixed signal circuits can heavily load the output of a NAND gate. An example of this type of digital circuit is an output buffer. Examples

of heavily loading mixed signal circuits include charge pumps and loop filters (e.g., digital phase-locked loops or DPLL). The capacitive load, C_L , for these circuits can be 1 pF or larger. It would be of definite interest to determine if the change in t_r of a NAND circuit, measured under the heavy C_L of the switch matrix technique, can be directly attributed to the oxide degradation of one MOSFET in the NAND gate. Theoretically, this might be possible by examining the well known relationship of t_r shown previously in Eq. (1). If a NAND gate is under a large load capacitance, which remains constant, then a change in R_{ch} can be directly related to a change in t_r . Hence, Eq. (1) can then be written in terms of a change in R_{ch} (ΔR_{ch}) given by:

$$\Delta t_r \propto \Delta R_{ch} C_L \quad (2)$$

or,

$$\Delta t_r \propto (R_{ch, \text{fresh}} - R_{ch, \text{wearout}}) C_L. \quad (3)$$

Consider the following case in which C_L can be increased or decreased prior to or after circuit operation but remains constant during circuit operation or measurement (i.e., a different output circuit on the NAND). A question arises as to whether or not the change in C_L produces a change in $\% \Delta t_r$ (where $\%$ signifies fractional percent). Insight to this question is gained by writing Eq. (1) in terms of $\% \Delta t_r$:

$$\% \Delta t_r \propto \frac{\Delta t_r}{t_{r, \text{fresh}}} \propto \frac{\Delta t_r}{R_{ch, \text{fresh}} C_L}. \quad (4)$$

Substituting Eq. (3) into (4) provides:

$$\begin{aligned} \% \Delta t_r &\propto \frac{(R_{ch, \text{fresh}} - R_{ch, \text{wearout}}) C_L}{R_{ch, \text{fresh}} C_L} \propto \frac{R_{ch, \text{fresh}} - R_{ch, \text{wearout}}}{R_{ch, \text{fresh}}} \\ &\propto \% \Delta R_{ch}. \end{aligned} \quad (5)$$

Eq. (5) reveals that $\% \Delta t_r$ is independent of C_L . The result of Eq. (5) is rather simplistic and may leave the reader with doubt to its outcome. Hence, SPICE simulations were performed that demonstrate, for changes in C_L ranging from 10 fF up to 1 nF (but holding C_L constant during each simulation), $\% \Delta t_r$ remains the same, Fig. 3.

Degradation was simulated in a single pMOSFET by increasing the threshold voltage parameter, V_{TH0} , of a 50 nm CMOS process BSIM 4 SPICE model to match the $\% \Delta V_{TH}$ increase observed in the experimental data following oxide wear out in a single pMOSFET. V_{TH0} was chosen because of its relationship to R_{ch} as shown later. The NAND circuit investigated in this study was simulated using LT SPICE. Voltage–time-domain simulations were performed for the NAND circuits using the capacitive load of the Switch Matrix Technique (i.e., approximately 900 pF). Fig. 4 illustrates the typical correlation between simulated and experimental results. The switch matrix technique is well suited to examine the reliability of simple integrated circuit building blocks (SICBB) since the C_L for this technique is about 900 pF (within the range of simulations) and remains constant throughout testing. We have also

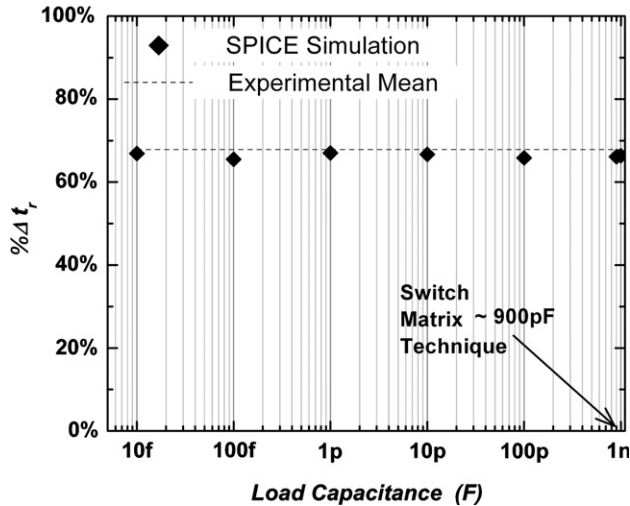


Fig. 3. SPICE simulation results showing $\% \Delta t_r$ as a function of C_L for NAND circuit configuration 1–3 (Table 1). Results indicate $\% \Delta t_r$ remains fairly constant within the range of 10 fF to 1 nF. It is interesting to note that simulation results for $\% \Delta t_r$ are near the mean value of experimental data obtained using the switch matrix technique. The arrow indicates the approximate C_L associated with the Switch Matrix Technique.

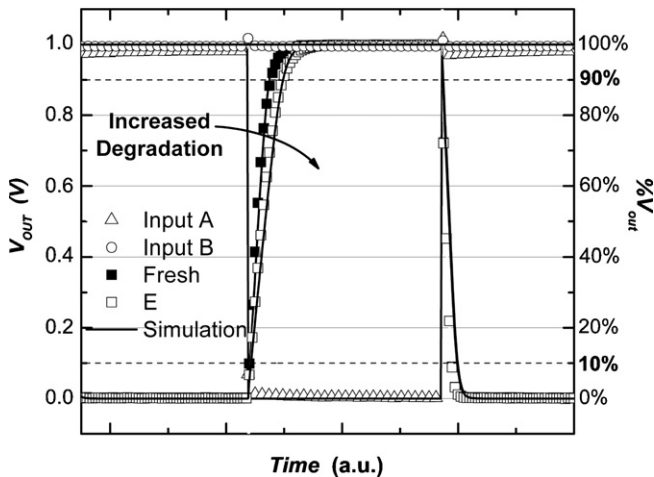


Fig. 4. Typical experimental and SPICE simulation voltage–time–domain ($V-t$) results for NAND circuit configuration 1–3 (Table 1). Only the fresh and stress cycle E response are shown. Experimental data are represented by the symbols while simulation data are shown as solid lines. Degradation was simulated in a single pMOSFET by increasing the threshold voltage parameter, V_{TH0} , of a 50 nm CMOS process BSIM 4 SPICE model to match the mean $\% \Delta V_{TH}$ increase observed in the experimental data following oxide wear out of a single pMOSFET. The NAND circuit investigated in this study was simulated using LT SPICE. The observed increase in $\% \Delta t_r$ of the simulation data is shown to correlate well with the observed increase in $\% \Delta t_r$ of the experimental results.

performed experiments in which the C_L on the NAND gate was reduced by nearly an order of magnitude and obtained the same results (within a standard deviation) as with the switch matrix technique.

Using the switch matrix technique, we examine the effect of oxide wear out in a pMOSFET on the functionality of a NAND logic circuit. It is shown for NAND

gates, which can be heavily loaded by circuits such as output buffers, charge pumps and loop filters, that pMOSFET oxide wear out is significantly disruptive to NAND gate performance.

3. Results

The NAND circuit and pMOSFET results reported include the $\% \Delta$ from fresh to wear out in terms of the mean value. The pMOSFET results are summarized in Table 2. For both the NAND circuit and the pMOSFET only the $\% \Delta$ mean is referenced in the following subsections.

3.1. NAND circuit

Following degradation of a single pMOSFET, both $V-t$ and VTCs are examined for configurations 1–3 and 2–1 (Table 1). These configurations are the only two configurations exhibiting effects from pMOSFET degradation as expected. Fig. 5 shows the NAND $V-t$ response for circuit configurations (a) 1–3 and (b) 2–1. The NAND $V-t$ response for Fig. 5a and b shows an increase in $\% \Delta t_r$ of approximately 68%, relative to the fresh response. Fig. 6 shows the NAND VTCs for configurations (a) 1–3 and (b) 2–1, in which a shift to the left, starting from the fresh condition, is observed in the voltage switching point ($\% \Delta V_{SP}$) by approximately 11% and 9%, respectively. Fig. 7 shows box plots with respect to stress cycle of (a) $\% \Delta t_r$ and (b) $\% \Delta V_{SP}$. The mean values of each box plot are connected by a solid line, indicating a gradual increase in mean values for each tested circuit with increased degradation as illustrated in Figs. 5 and 6. A gradual increase in the value of the interquartile range with increased oxide wear out is also observed.

3.2. pMOSFET

After 3000 s of CVS, the pMOSFET DC characteristics show a decrease in $\% \Delta I_{D,max}$ (Fig. 8) by 43%. Fig. 9 reveals an increase in $\% \Delta V_{TH}$ by 23%, and a decrease in $\% \Delta G_{M,max}$ (inset of Fig. 9) by 26%. Additionally, a decrease in $\% \Delta I_{off}$ by 82% is observed (Fig. 10). The $\% \Delta g_{sdm}$ in Fig. 11 is shown to decrease by 30% (measured at $V_{SG} = V_{DD} = 1$ V). In Fig. 12, an increase is observed in $\% \Delta R_{ch}$ of approximately 44%.

Table 2
pMOSFET device statistics

$I-V$ parameter	Mean (%)	Standard deviation (%)
$\% \Delta I_{D,max}$	43	8
$\% \Delta V_{TH}$	23	5
$\% \Delta G_{M,max}$	26	3
$\% \Delta I_{off}$	82	7
$\% \Delta g_{sdm}$	30	8

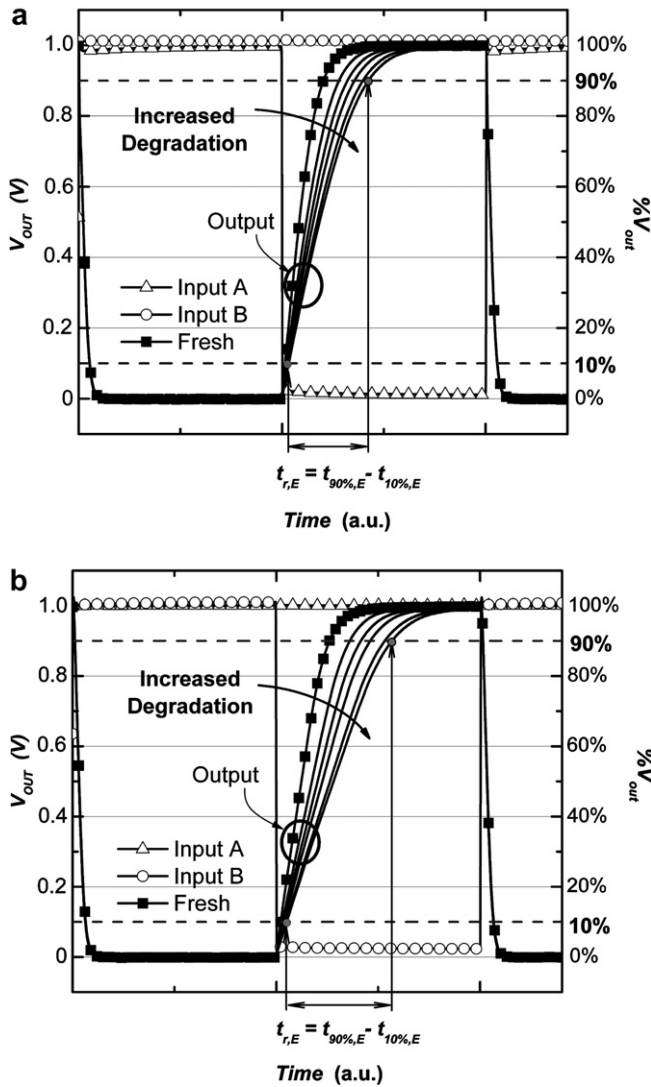


Fig. 5. Typical voltage–time-domain ($V-t$) results for the NAND circuit for fresh through stress cycle E (i.e. Region Investigated in Fig. 1). Results show an increase in t_r of approximately 68% with increasing wear out, in which t_r is measured as the difference in time from 90% to 10% of the final output voltage [19,20]. Wear out in one pMOSFET significantly affects the rise time (t_r) as shown for configurations (a) 1–3 and (b) 2–1. The equation for t_r is demonstrated for the stress cycle E curve.

4. Discussion

4.1. NAND circuit

The method that was chosen for testing the NAND gate induces a pulsed waveform on one input while applying a constant voltage to the other input. Thus, simplifying the experiment by isolating the switching transistors in the NAND gate to one pMOSFET and one nMOSFET (cases A and B described by Taur and Ning) [24]. This method prevents both pMOSFETs from switching simultaneously and allows for easier analysis of the impact of the degraded pMOSFET on the NAND circuit response. It is shown following stress of a single pMOSFET, the

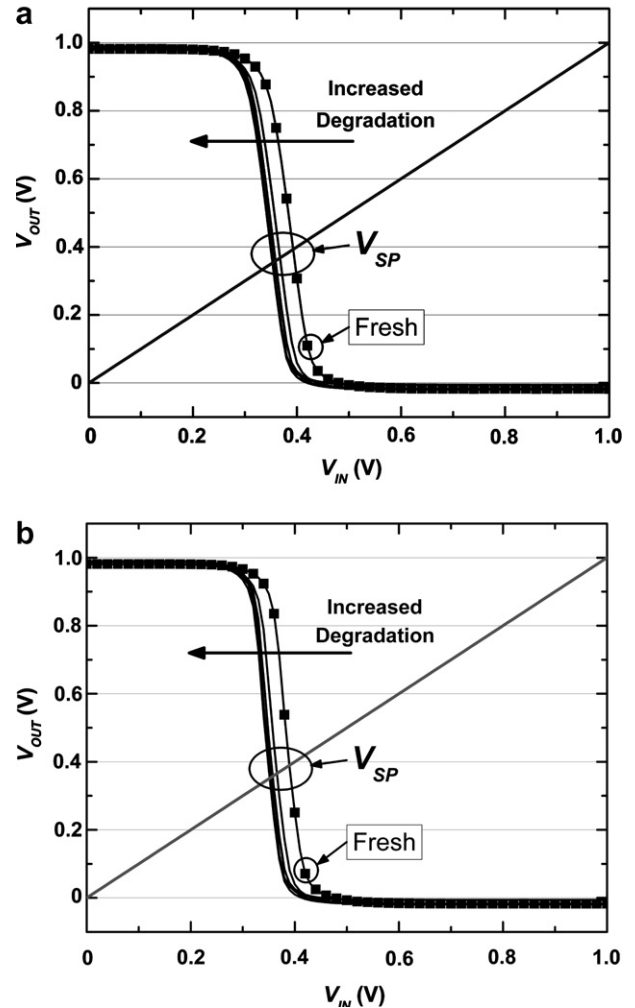


Fig. 6. Typical voltage transfer characteristics (VTCs) results for the NAND gate from fresh to stress cycle E . Effects of wear out in one pMOSFET are shown for configurations (a) 1–3 and (b) 2–1, in which a shift to the left in the voltage switching point (V_{SP}) of approximately (a) 11% (b) and 9% are observed. V_{SP} is defined as the switching point voltage when the line, $V_{out} = V_{in}$, intersects the data.

degree of degradation observed in the NAND time-domain response is more significant than the degradation exhibited in the VTCs under equivalent test conditions (Figs. 5 and 6).

Examining the data in Fig. 5 demonstrates that only t_r of the NAND gate is affected, while the fall time (t_f) remains unchanged (Fig. 5). As reported by Stutzke et al., a degraded pMOSFET affects only the t_r [3], hence a change in t_r is not expected, nor is it observed. This can be explained by realizing that the pMOSFET is the “pull-up” device and the nMOSFET is the “pull-down” device, as described by Taur and Ning [24]. Furthermore, comparison of the $\% \Delta t_r$ results for configuration 1–3 (Fig. 5a) to the $\% \Delta t_r$ results for configuration 2–1 (Fig. 5b) reveals that a single degraded pMOSFET has an equivalent effect on NAND circuit performance in the $V-t$ domain regardless of circuit configuration. This can be explained by realizing that by holding one input of the

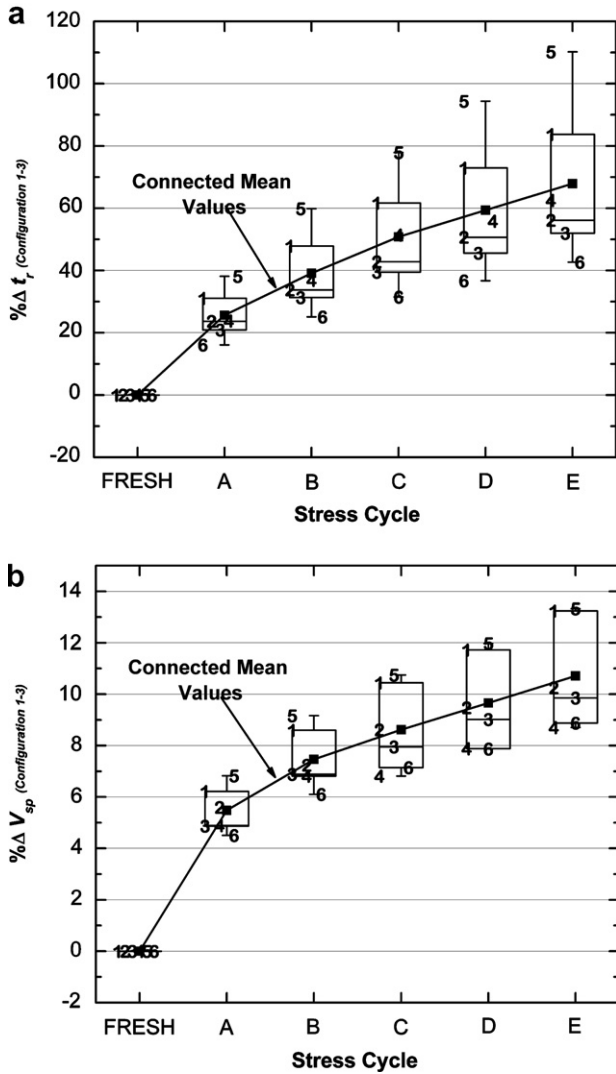


Fig. 7. Box plots of (a) voltage–time-domain ($V-t$) and (b) voltage transfer characteristics (VTCs) for configuration 1–3 versus stress cycle. The numbers illustrate the different circuits tested (i.e., all four MOSFETs used to construct the NAND circuit are different and unstressed before testing). Each individual box plot has a range from the minimum measured value to the maximum measured value. The box represents the interquartile range. The mean values of each individual box plot are depicted by a solid square and are connected by a solid line. The median is illustrated by a horizontal solid line in the box. Configuration 2–1, not shown, yields comparable results. The $\% \Delta t_r$ from fresh to stress cycle E for this configuration is approximately 68% while the $\% \Delta V_{sp}$ from fresh to stress cycle E is only 11% (by mean). A gradual increase in the value of the interquartile range with increased stress time is observed for both (a) $\% \Delta t_r$ and (b) $\% \Delta V_{sp}$.

NAND gate at VDD while the other input is pulsed, the pull-up operation of a two input NAND gate is similar to that of a CMOS inverter [24]. Hence, for both configurations 1–3 and 2–1, the impact of single pMOSFET oxide wear out on the NAND logic gate performance in the $V-t$ domain is comparable to findings reported in similar work involving the Inverter logic circuit [4]. Moreover, the data in Fig. 5 may be examined statistically over the stress cycles as shown in Fig. 7a. Statistical examination of the data

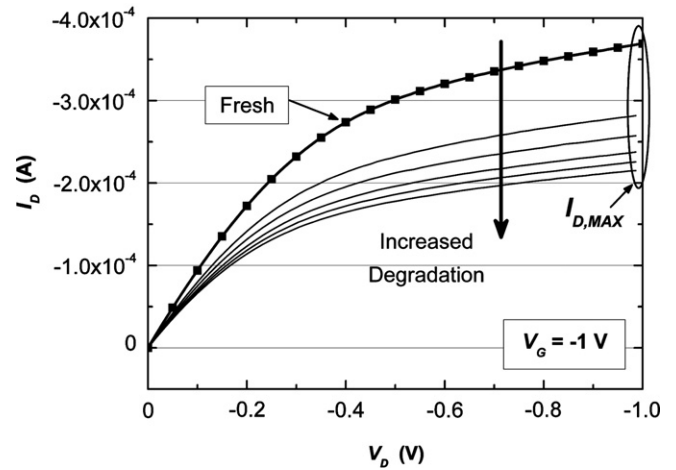


Fig. 8. Typical pMOSFET drain current versus drain voltage ($I_D - V_D$) results for fresh through stress cycle E showing a decrease in $I_{D,max}$ of approximately 43% with increasing wear out. $I_{D,max}$ data is measured at $V_D = V_{DD}$ (circled). The gate voltage is held constant at -1 V throughout the test.

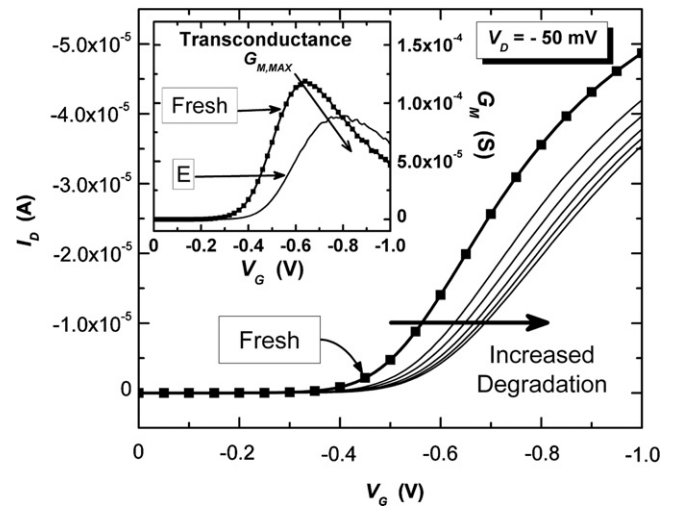


Fig. 9. Typical pMOSFET linear drain current versus gate voltage (linear $I_D - V_G$) results for fresh through stress cycle E, in which an increase in threshold voltage (V_{TH}) of approximately 23% is observed from fresh to stress cycle E. The inset illustrates that the corresponding maximum transconductance ($G_{M,max}$) decreases by approximately 26% and shifts to more negative voltages with increased wear out (only fresh and stress cycle E are presented). Throughout the test, drain voltage is held constant at -50 mV . V_{TH} is measured using the linear extrapolation method [22].

reveals valuable information concerning trends in the circuit $V-t$ response (Fig. 7a). The data in Fig. 7a indicate the $\% \Delta t_r$ increases steadily and substantially for each circuit. For all circuits tested, the same trend in $\% \Delta t_r$ is observed, which is a sublinear increase in $\% \Delta t_r$ with increasing stress cycle.

A similar correlation can be made for the NAND VTCs from Fig. 6, in which a leftward shift of the V_{sp} is directly related to a decrease in pMOSFET performance. This effect was also observed for inverters in which a degraded

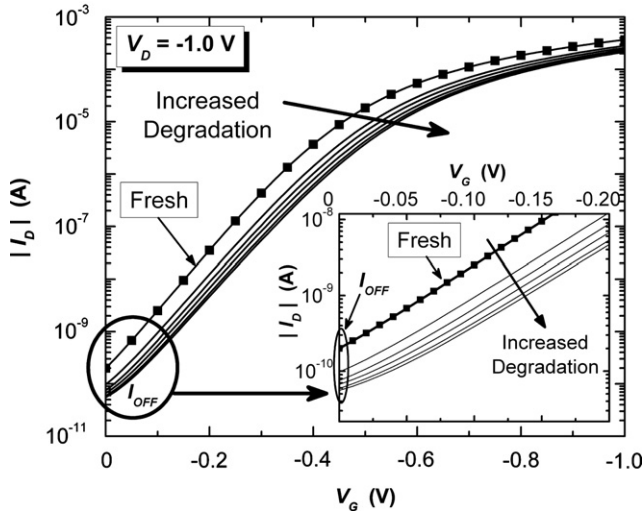


Fig. 10. Typical pMOSFET logarithm drain current ($\log I_D$) versus gate voltage (V_G) results for fresh through stress cycle E, showing a decrease of approximately 82% in off-current (I_{OFF}) after induced wear out. The I_{OFF} data is encircled and emphasized in the inset plot. Throughout the test, the drain voltage is held constant at -1 V.

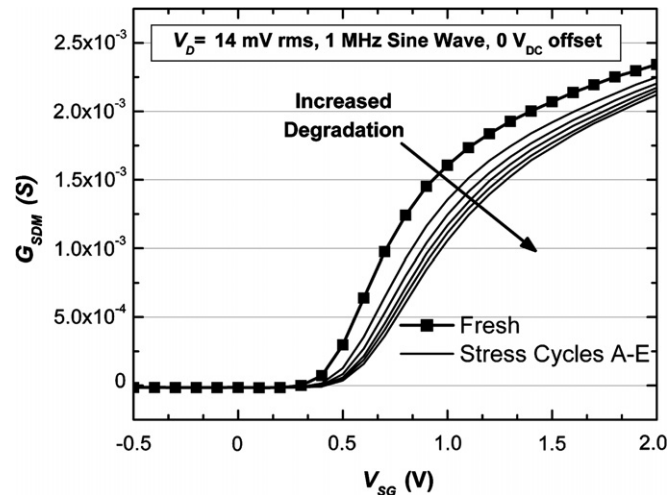


Fig. 11. Typical pMOSFET small-signal conductance measurement results for fresh through stress cycle E showing a decrease of approximately 30% in source-to-drain conductance (g_{sdm}) after induced wear out. The $\% \Delta g_{sdm}$ results reported are measured at $V_{SG} = V_{DD} = 1$ V. Throughout the test the drain voltage is held at a 0 V_{DC} bias with a 14 mV_{rms} sinusoidal signal at a frequency of 1 MHz superimposed.

pMOSFET and undamaged nMOSFET shifted the V_{SP} to the left while a degraded nMOSFET and undamaged pMOSFET shifted the V_{SP} to the right [4,6]. Additionally, comparison of the $\% \Delta V_{SP}$ data for configurations 1–3 and 2–1 (Fig. 6a and b) demonstrates a single degraded pMOSFET has a similar effect on NAND circuit performance in the DC domain regardless of circuit configuration. This can also be explained by realizing that by holding one input of the NAND gate at V_{DD} while the other input is pulsed the pull-down operation of a two input NAND gate is similar to that of a CMOS inverter [24]. However,

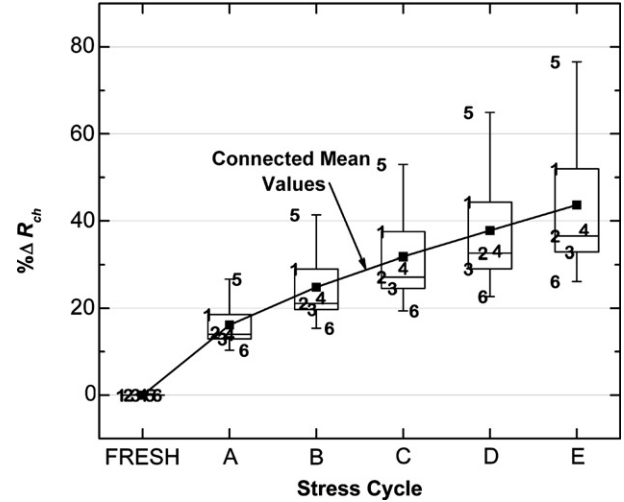


Fig. 12. Box plot of $\% \Delta R_{ch}$ versus stress cycle, indicating a gradual increase in channel resistance with increased wear out. The numbers illustrate the different pMOSFETs which were degraded in this study. MOSFET numbers correlate to NAND logic circuit numbers in Fig. 7. The $\% \Delta R_{ch}$ from fresh to stress cycle E is approximately 44% (by mean). Each individual box plot has a range from the minimum measured value to the maximum measured value. The box represents the interquartile range. The mean values of each individual box plot are depicted by a solid square and are connected by a solid line. The median is illustrated by a horizontal solid line in the box. A gradual increase in the value of the interquartile range is observed with increasing stress time.

it is important to note that configuration 2–1 is most comparable to the CMOS Inverter as VTC results for configuration 1–3 could be influenced by the body effect associated with stacked nMOSFET devices [24]. Hence, the observed $\% \Delta V_{SP}$ for configuration 2–1 is most comparable to the $\% \Delta V_{SP}$ reported in similar work involving the Inverter logic circuit [4]. Statistical examination of the data in Fig. 6a provides the box plots in Fig. 7b where the $\% \Delta V_{SP}$ data for each circuit are shown over the stress cycles. The $\% \Delta V_{SP}$ depicts a sublinear increase as well, thus further suggesting the validity of the trends in both $\% \Delta t_r$ and $\% \Delta V_{SP}$ with stress time.

The evolution of $\% \Delta t_r$ and $\% \Delta V_{SP}$ may be described by the slope of the curves which connect the box plot mean values as shown in Fig. 7a and b. Initially, the slopes of these curves are large but decrease to a relatively constant value. This tendency correlates to the pMOSFET gate leakage current progression with respect to degradation encircled in the “Region Investigated” in Fig. 13. The first cycle of wear out shows the greatest change in gate leakage current while subsequent wear out exhibits less leakage current changes. It is interesting to note that the $\% \Delta t_r$ increase is a factor of four or more greater than that observed for the $\% \Delta V_{SP}$ indicating that the circuit operation in the time domain is more affected by gate oxide wear out than for DC operation. Since a significant portion of circuit operation is in the time-domain, the greater sensitivity of $\% \Delta t_r$ to gate oxide wear out suggests that gate oxide wear out is more detrimental to digital circuit operation than to analog operation.

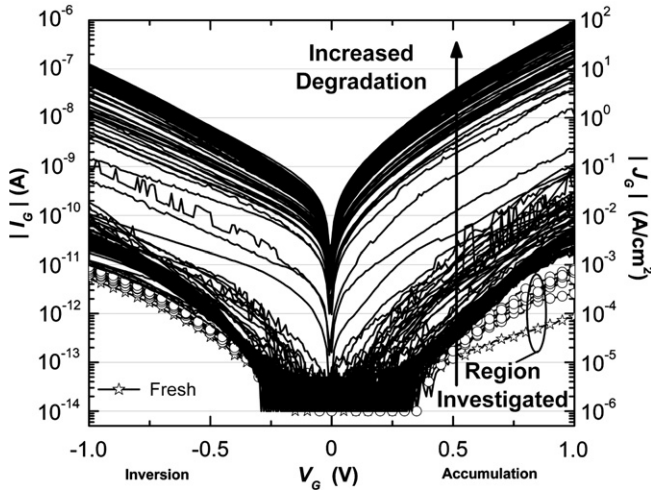


Fig. 13. Log plot of the gate current versus gate voltage response for the degraded pMOSFET corresponding to the CVS plot shown in Fig. 2. The Region Investigated for wear out (encircled fresh $I_G - V_G$ curve (stars) and the consecutive cycles of degradation A–E (circles)) correlates to the Region Investigated in Fig. 2. The full range of oxide degradation is shown to highlight the low-leakage regime investigated in this study. The pMOSFETs used in this study were not stressed beyond the Region Investigated. The low-leakage regime suggests that a traditional oxide breakdown event (i.e., SBD or HBD) is not being induced in the pMOSFETs used in this study [18]. The arrow indicates the progression of increased degradation. It should be noted that both inversion and accumulation modes indicate increased degradation.

Similar observations were reported by Cheek et al. following inverter circuit analysis [6]. In addition, the degradation of the NAND $V-t$ response with increased wear out reported in Section 3.1 are supported by the simulation work of Carter et al. in which GOB is simulated and the result is an increase in time delay for the NAND gate time-domain response [10].

4.2. pMOSFET

The evidence presented in Section 4.1 indicates that pMOSFET wear out causes a significant change in NAND gate circuit response. Consequently, the pMOSFET characteristics are examined to establish the cause of the large change in t_r . The $I_G - V_G$ data in Fig. 13 are substantiated by the Region Investigated highlighted in Fig. 1 where wear out is evident. A potential link between circuit performance and MOSFET degradation is that of t_r and R_{ch} (Eqs. (1) and (5)). To this end, R_{ch} is investigated experimentally. To obtain the values for $\% \Delta R_{ch}$, an approach similar to that provided by Kong et al. [23] was applied in which an equation for g_{sdm} is derived. Kong's derivation for g_{sdm} , calculated from the DC drain current equation of an nMOSFET, is based upon the gradual channel approximation [23]. The gradual channel approximation remains valid for this study as only a small AC signal with a 0 V DC bias is applied to the drain when g_{sdm} is measured. Therefore, a similar derivation for the case of a pMOSFET results in

$$g_{sdm} = \frac{1}{R_{SD} + \frac{1}{\beta(V_{SG} + V_{TH})}}, \quad (6)$$

where,

$$R_{ch} = \frac{1}{\beta(V_{SG} + V_{TH})} \quad (7)$$

and,

$$\beta = \frac{\mu_{eff} C_{OX} W_{eff}}{L_{eff}}. \quad (8)$$

R_{SD} is the total parasitic source and drain resistance measured in series with R_{ch} . It can be assumed R_{SD} is small compared to R_{ch} [25,26] and remains fairly constant after CVS, as the majority of the pMOSFET degradation occurs in the channel [21]. Therefore, Eq. (4) can be reduced to

$$g_{sdm} \approx \frac{1}{R_{ch}} \quad (9)$$

or equivalently,

$$R_{ch} \approx \frac{1}{g_{sdm}}. \quad (10)$$

A correlation between $\% \Delta R_{ch}$ and g_{sdm} can be derived from Eq. (10). ΔR_{ch} can be written as

$$\Delta R_{ch} \approx \frac{1}{g_{sdm, fresh}} - \frac{1}{g_{sdm, wearout}}. \quad (11)$$

Using a common denominator, (11) can be written as

$$\Delta R_{ch} \approx \frac{-\Delta g_{sdm}}{g_{sdm, fresh} g_{sdm, wearout}}. \quad (12)$$

Dividing by $R_{ch, fresh}$ to convert (12) to fractional percent change results in

$$\% \Delta R_{ch} \approx \frac{\Delta R_{ch}}{R_{ch, fresh}} \approx \frac{-\Delta g_{sdm}}{g_{sdm, wearout}}. \quad (13)$$

Using Eq. (13), $\% \Delta R_{ch}$ was calculated using the small-signal conductance data. A statistical examination of the $\% \Delta R_{ch}$ data (Fig. 12) reveals a sublinear increase similar to the $\% \Delta t_r$ data (Fig. 7a). The evolution of $\% \Delta R_{ch}$ may also be described by the slope of the line connecting the box plot mean values (Fig. 12). Initially, the slope is large but decreases to a shallower value. However, it is most interesting to note that the $\% \Delta R_{ch}$ trends for the devices (Fig. 12) are comparable with the $\% \Delta t_r$ trends for the correlating circuits (Fig. 7a). To further discern the relationship between $\% \Delta t_r$ and $\% \Delta R_{ch}$ observed in Fig. 7a and Fig. 12, both the $\% \Delta t_r$ data and $\% \Delta R_{ch}$ data are plotted in Fig. 14. The linear fit of the data in Fig. 14 shows that $\% \Delta t_r$ is directly proportional to $\% \Delta R_{ch}$ through the relationship,

$$\% \Delta t_r = 1.52 \times \% \Delta R_{ch}. \quad (14)$$

The graphical relation observed in Fig. 14 demonstrates the validity of Eqs. (1) and (5) as well as the correlation between the trends illustrated in Fig. 7a and Fig. 12. Hence,

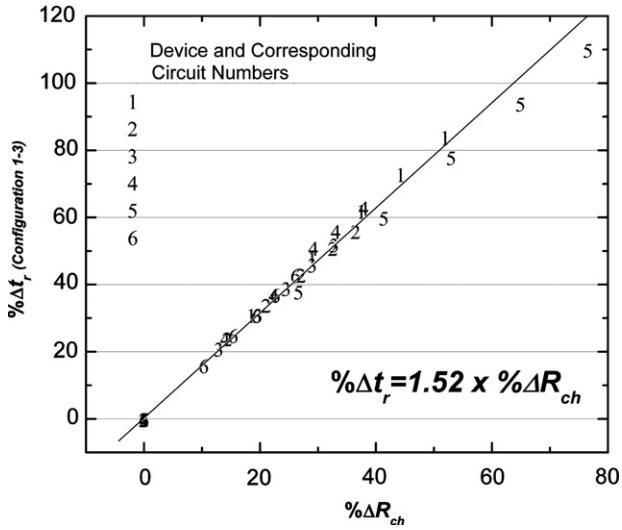


Fig. 14. A linear relationship between $\% \Delta t_r$ and $\% \Delta R_{ch}$ is demonstrated for NAND logic configuration 1–3. Similar results were observed for configuration 2–1. The six degraded pMOSFETs used in this study are represented numerically and correspond to the NAND logic circuit numbers in Fig. 7. A linear increase in $\% \Delta t_r$ as a function of $\% \Delta R_{ch}$ is observed for each device. A linear fit (line) to the mean values of each stress cycle is included to highlight the proportionality expressed in Eq. (5). The equation of the linear fit is expressed in (14).

the change in channel resistance in the pMOSFET due to oxide degradation directly affects the rise time of the NAND logic gate.

Further insight into the degraded parameters affecting R_{ch} is gained by following the derivation of Kong et al. relating $g_{sdm} / \sqrt{dg_{sdm}/dV_{SG}}$ as a linear function of gate voltage [23]. In the case of the pMOSFET, this relationship is expressed as

$$\frac{g_{sdm}}{\sqrt{\frac{dg_{sdm}}{dV_{SG}}}} = \sqrt{\beta_0}(V_{SG} + V_{TH}), \quad (15)$$

where the zero gate-field gain factor, β_0 , is proportional to β through the well known relationship shown in Eq. (16) [27],

$$\mu_{eff} = \frac{\mu_0}{1 + \theta(V_{SG} + V_{TH})} \quad (16)$$

and θ is the gate-field mobility reduction factor. When the g_{sdm} data are plotted according to Eq. (15) and a linear fit is applied to the various stress cycles (Fig. 15), it is observed that the slope of the linearization (i.e., $\sqrt{\beta_0}$) decreases with increased stress time. Furthermore, the shift in the x -intercept (i.e., V_{TH}) is approximately equal to the V_{TH} shift measured using the linear extrapolation method (Fig. 9). Therefore, the results of the small-signal conductance measurement (Figs. 11 and 15) and the relationship expressed in Eq. (15) are substantiated by the data in Fig. 9, where a decrease in $G_{M,max}$ and shift in V_{TH} are observed. Hence, the increase in R_{ch} can be partly attributed to a decrease in μ_{eff} , in accordance with Eq. (16). Since this study focuses on circuit response to MOSFET degradation, further

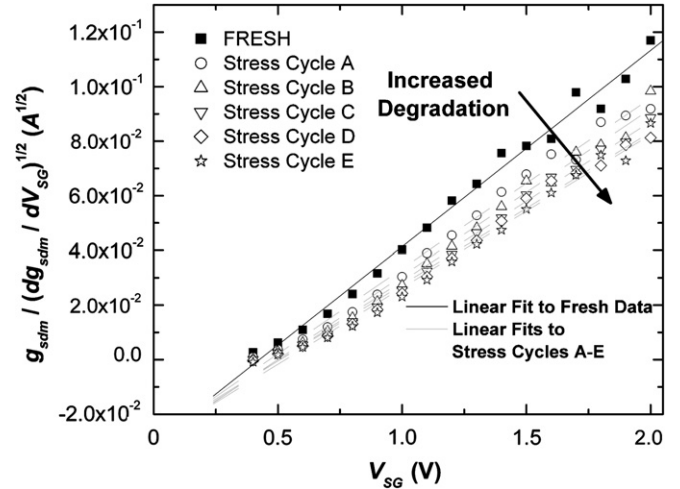


Fig. 15. Typical pMOSFET small-signal conductance measurement results for fresh through stress cycle E linearized through Eq. (12). The decrease in the slope of the linear extrapolations indicates a decrease in $\beta_0^{1/2}$. Also noted is a shift in the x -axis intercept of approximately 22%, which correlates well with the $\% \Delta V_{TH}$ measured through the linear extrapolation method as demonstrated in Fig. 9.

investigation in the degradation mechanisms affecting R_{ch} remains a topic that is beyond the scope of this paper.

5. Conclusions

Using a switch matrix technique, the results reported in this study show gate oxide wear out in one pMOSFET of a NAND logic circuit substantially degrades the circuit V - t domain response and the VTCs. Additionally, it was found the NAND gate response in the V - t domain is comparatively worse than the DC response. We have also proposed and shown the switch matrix technique can be employed in conjunction with a small-signal conductance measurement in characterizing the reliability of SICBBs, despite a relatively heavy capacitive load. A correlation between NAND logic circuit performance and degradation of pMOSFET parameters is established through analyses of $\% \Delta t_r$ and $\% \Delta R_{ch}$. Ultimately, the changes in t_r may dramatically affect the ability of the NAND gate to execute logic properly, particularly in applications requiring high switching speeds.

Acknowledgements

The authors would like to thank Gennadi Bersuker and Rino Choi from SEMATECH, Inc. as well as Betsy Cheek, Josh Keipert and Terry Gorseth from Boise State University for their contributions to this work. Funding for the project was supported in part by DARPA Contract #N66001-01-C-80345, NIH INBRE #P20RR16454, and NSF MRI Award #0216312. D. Estrada would like to acknowledge the McNair Scholars Program for partial support.

References

- [1] Rodriguez R, Stathis JH, Linder BP. A model for gate-oxide breakdown in CMOS inverters. *IEEE Electron Dev Lett* 2003;24:114–6.
- [2] Rodriguez R, Stathis JH, Linder BP. Modeling and experimental verification of the effect of gate oxide breakdown on CMOS inverters. Presented at IEEE international reliability physics symposium; 2003.
- [3] Stutzke N, Cheek BJ, Kumar S, Baker RJ, Moll AJ, Knowlton WB. Effects of circuit-level stress on inverter performance and MOSFET characteristics. Presented at IEEE international integrated reliability workshop; 2003.
- [4] Ogas ML, Southwick RG, Cheek BJ, Baker RJ, Gennadi B, Knowlton WB. Survey of oxide degradation in inverter circuits using 2.0 nm MOS devices. Presented at IEEE international integrated reliability workshop; 2004.
- [5] Huang HM, Ko CY, Yang ML, Liao PJ, Wang JJ, Oates A, Wu K. Gate oxide multiple soft breakdown (multi-SBD) impact on cmos inverter. Presented at IEEE international reliability physics symposium; 2004.
- [6] Cheek B, Stutzke N, Kumar S, Baker RJ, Moll AJ, Knowlton WB. Investigation of circuit-level oxide degradation and its effect on CMOS inverter operation and MOSFET characteristics. Presented at IEEE international reliability physics symposium; 2004.
- [7] Rodriguez R, Stathis JH, Linder BP, Joshi RV, Chuang CT. Influence and model of gate oxide breakdown on CMOS inverters. *Microelectron Eng* 2003;43:1439–44.
- [8] Rodriguez R, Stathis JH, Linder BP. Effect and model of gate oxide breakdown on CMOS inverters. *Microelectron Eng* 2004;72:34–8.
- [9] Ogas ML, Price PM, Kiepert J, Baker RJ, Bersuker G, Knowlton WB. Degradation of rise time in NAND gates using 2.0 nm gate dielectrics. Presented at presented at IIRW. Fallen Leaf Lake, CA; 2005.
- [10] Carter JR, Ozev S, Sorin DJ. Circuit-level modeling for concurrent testing of operational defects due to gate oxide breakdown. Presented at IEEE design, automation, and test in Europe; 2005.
- [11] Hawkins C, Keshavarzi A, Segura J. CMOS IC nanometer technology failure mechanisms. Presented at IEEE custom integrated circuits conference; 2003.
- [12] Denais M, Huard V, Parthasarathy C, Ribes G, Perrier F, Revil N, et al. Interface trap generation and hole trapping under NBTI and PBTI in advanced CMOS technology with a 2-nm gate oxide. *IEEE Trans Dev Mater Reliab* 2004;4:715–22.
- [13] Stathis JH, Zafar S. The negative bias temperature instability in MOS devices: a review. *Microelectron Reliab* 2006;46:270–86.
- [14] Haggag A, Liu N, Menke D, Moosa M. Physical model for the power-law voltage and current acceleration of TDDB. *Microelectron Reliab* 2005;45:1855–60.
- [15] Weir BE, Silverman PJ, Monroe D, Krisch MA, Alam MA, ALers GB, Sorsch TW, Timp GL, Baumann F, Liu CT, Ma Y, Hwang D. Ultra-thin gate dielectrics: they break down, but do they fail? Presented at IEEE international electron devices meeting; 1997.
- [16] Lin HC, Lee DY, Huang TY. Breakdown modes and their evolution in ultra-thin gate oxides. *Jpn J Appl Phys* 2002;41:5957–63.
- [17] Cester A, Paccagnella A, Ghidini G, Deleonibus S, Guegan G. Collapse of MOSFET drain current after soft breakdown. *IEEE Trans Dev Mater Reliab* 2003;4:63–72.
- [18] Dumin DJ. Oxide wearout, breakdown, and reliability. *Int J High Speed Electron Syst* 2001;11:617–718.
- [19] Uyemura JP. The rise time. In: *Introduction to VLSI circuits and systems*. New York: John Wiley & Sons, Inc.; 2002. p. 250–3.
- [20] Baker RJ. The RC delay through an N-well. In: *CMOS: circuit design, layout, and simulation*. IEEE Press Wiley; 2005. p. 49–52.
- [21] Crupi F, Kaczer B, Degraeve R, Keergietter AD, Groeseneken G. A comparative study of the oxide breakdown in short-channel nMOS-FETs and pMOSFETs stressed in inversion and in accumulation regimes. *IEEE Trans Dev Mater Reliab* 2003;3.
- [22] Schroder DK. Threshold voltage. In: *Semiconductor material and device characterization*, 3rd ed.; 2006. p. 222–25.
- [23] Kong FCJ, Yeow YT, Yao ZQ. Extraction of MOSFET threshold voltage, series resistance, effective channel length, and inversion layer mobility from small-signal channel conductance measurement. *IEEE Trans Electron Dev* 2001;48:2870–4.
- [24] Taur Y, Ning TH. CMOS performance factors. In: *Fundamentals of Modern VLSI Devices*. Boston: Cambridge University Press; 1998. p. 224–91.
- [25] Taur Y. MOSFET channel length: extraction and interpretation. *IEEE Trans Electron Dev* 2000;47.
- [26] Ozturk MC. Source/drain junctions and contacts for 45 nm CMOS and Beyond. In: Presented at international conference on characterization and metrology for ULSI technology; 2005.
- [27] Fu KY. Mobility degradation due to the gate field in the inversion layer of MOSFETs. *IEEE Electron Dev Lett* 1982;EDL-3:292–3.